Influence of As on the formation of mask-edge defects during stressed solid phase epitaxy in patterned Si wafers

N. G. Rudawski, K. S. Jones, and R. G. Elliman

Citation: Journal of Vacuum Science & Technology B **26**, 435 (2008); doi: 10.1116/1.2775459
View online: http://dx.doi.org/10.1116/1.2775459
View Table of Contents: http://scitation.aip.org/content/avs/journal/jvstb/26/1?ver=pdfcov
Published by the AVS: Science & Technology of Materials, Interfaces, and Processing

Articles you may be interested in

Defect mitigation by ion induced amorphousization and solid-phase epitaxy
AIP Conf. Proc. **1525**, 204 (2013); 10.1063/1.4802320

Insights into solid phase epitaxy of ultrahighly doped silicon
J. Appl. Phys. **108**, 013513 (2010); 10.1063/1.3408556

Effect of uniaxial stress on solid phase epitaxy in patterned Si wafers
Appl. Phys. Lett. **89**, 082107 (2006); 10.1063/1.2337994

Effect of stress on the evolution of mask-edge defects in ion-implanted silicona)
J. Vac. Sci. Technol. B **24**, 446 (2006); 10.1116/1.2162566

Nickel distribution in crystalline and amorphous silicon during solid phase epitaxy of amorphous silicon
J. Appl. Phys. **84**, 6644 (1998); 10.1063/1.369039

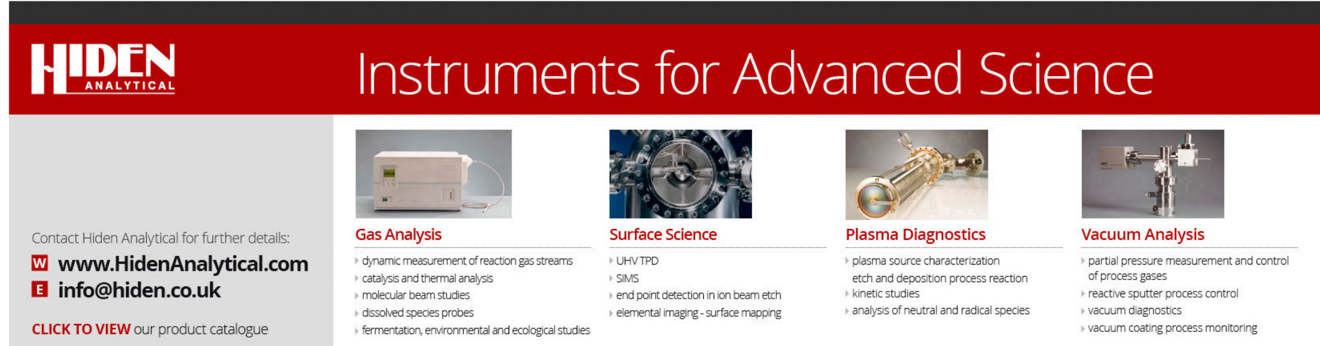

Redistribution subject to AVS license or copyright; see http://scitation.aip.org/termsconditions. Download to IP: 130.56.106.27 On: Wed, 21 Oct 2015 04:11:12

Influence of As on the formation of mask-edge defects during stressed solid phase epitaxy in patterned Si wafers

N. G. Rudawski[a] and K. S. Jones
Department of Materials Science and Engineering, University of Florida, Gainesville, Florida 32611-6400

R. G. Elliman
Electronic Materials Engineering Department, Research School of Physical Sciences and Engineering, Australian National University, Canberra, ACT 0200, Australia

(Received 30 May 2007; accepted 30 July 2007; published 1 February 2008)

The influence of As on the evolution of mask-edge defects during stressed solid phase epitaxy of two-dimensional Si^+ pre-amorphized regions in patterned Si wafers was examined. Mask-edge defects ~60 nm deep formed at 525 °C for As^+ implant energies of 7.5–50 keV with peak As concentration of $\sim 5.0\times 10^{20}$ cm^{-3}. Defect formation was attributed to an As-enhanced [110] regrowth rate relative to the [001] regrowth rate creating an amorphous/crystalline interface geometry favorable for defect formation. The similarity of mask-edge defect depths with As^+ implant energy was attributed to surface retardation of [110] regrowth in shallow implants and enhanced [001] regrowth in deeper implants. Results indicate stress effects on regrowth rates are small compared to dopant effects. © *2008 American Vacuum Society.* [DOI: 10.1116/1.2775459]

I. INTRODUCTION

It is known that pre-amorphization followed by subsequent solid phase epitaxy (SPE) of amorphized (α) Si created via ion-implantation can produce shallower junctions with active dopant concentrations in excess of substitutional solubility.[1–3] However, mask-edge defect formation in two-dimensional α-Si regions used for source and drain regions resulting from anisotropic SPE rates can severely degrade device performance.[4–6] Interestingly, it was shown that stress applied via patterning and external mechanical sources can influence the formation of these defects in regions amorphized with non-dopant species.[7–9] This stems from the observation that SPE rates are affected by stress.[10,11] However, while it is known that stress can influence defect formation via SPE, it is unclear whether the addition of dopant atoms affects a two-dimensional SPE process when stress is applied. Past studies investigating mask-edge defect formation utilized dopant species with nonuniform concentrations for creating α-Si layers.[12,13] Furthermore, since it is well known that dopant atoms cause large enhancements to the rate of SPE, it is possible that this influenced the shape of the regrowing α/crystalline interface.[14–16] In addition, it is unclear what effects dopants have on SPE for crystal orientations other than (001) and this may also be a contributing factor in the evolution of the regrowing interface. Furthermore, in the case of As^+-implantation below saturation but above solubility, dislocation loops form at the projected range (R_p) and it is unclear if the formation of these defects affects mask-edge defect formation.[17–20] Thus, the goal of this study is to determine the effect stress on SPE and mask-edge defect formation in two-dimensional α-Si regions implanted with a nonuniform As concentration.

[a]Electronic mail: ngr@ufl.edu

II. EXPERIMENT

For this study, 750-μm-thick patterned (001) Si wafers were used. The patterning consisted of $\sim 0.6\times 0.6$ μm^2 structures aligned along $\langle 110\rangle$ in-plane directions with 150 nm of Si_3N_4 on 10 nm of SiO_2 with ~0.3 μm of unmasked area between adjacent structures. All samples were Si^+-implanted at 20 and 60 keV with doses of 1×10^{15} cm^{-2} to produce an α-Si layer ~120 nm deep. Subsequently, some samples were additionally implanted with As^+ using energies of 7.5, 15, 30, or 50 keV with doses of 5.0×10^{14}, 7.3×10^{14}, 1.1×10^{15}, or 1.6×10^{15} cm^{-2}, respectively. These combinations were utilized to produce a peak As concentration of $\sim 5.0\times 10^{20}$ cm^{-3} at different depths as predicted using simulations.[21] Samples were annealed at 525 °C in an N_2 ambient for times of 0.8–3.0 h. Anneal times were chosen so that the SPE process was observed after half the annealing time required for completion ($t_{0.5}$) and after the full time required for completion ($t_{1.0}$). The anneal times were estimated based on the [001] SPE rate as enhanced by the presence of As and stress.[4,9,14] Bright-field (BF) cross-sectional transmission electron microscopy (XTEM) imaging using a g_{022} two-beam condition was used to image the regrowth of the α-Si layers and the formation of mask-edge defects. Specimens were prepared via focused ion beam milling.

III. RESULTS

Figure 1 displays XTEM images of the evolution of the SPE process at 525 °C in Si^+-implanted square structures with and without the patterning. The as-implanted samples are shown in the BF XTEM images in Figs. 1(a) and 1(d) and exhibit an α/crystalline interface with rounded corners beneath the SiO_2/Si_3N_4 mask edges. When the patterning was removed (unstressed) via HF etching and the samples annealed for $t_{0.5}=1.5$ h, the [110] and [001] SPE fronts con-

Redistribution subject to AVS license or copyright; see http://scitation.aip.org/termsconditions. Download to IP: 130.56.106.27 On: Wed, 21 Oct 2015 04:11:12

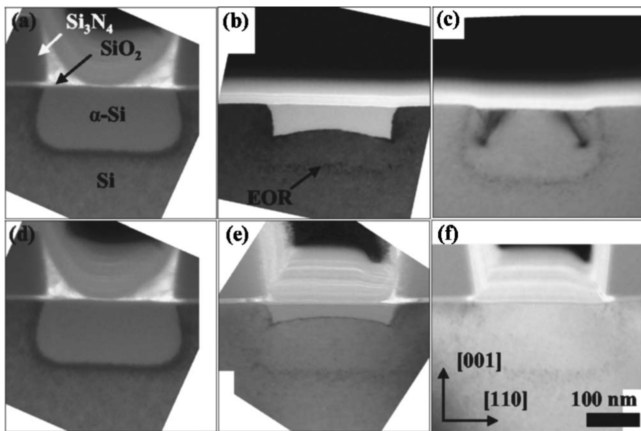

FIG. 1. BF XTEM images of Si^+-implanted samples annealed at 525 °C: (a) as-implanted, (b) annealed for $t_{0.5}$=1.5 h unstressed, (c) annealed for $t_{1.0}$=3.0 h unstressed, (d) as-implanted, (e) annealed for $t_{0.5}$=1.5 h with stress, and (f) annealed for $t_{1.0}$=3.0 h with stress.

verge at a depth of ~60 nm as shown in Fig. 1(b). In contrast, when the patterning was left intact (stressed) and the sample annealed to $t_{0.5}$=1.5 h, shown in Fig. 1(e), convergence is delayed until the [001] α/crystalline interface was ~20 nm deep. After annealing for $t_{1.0}$=3.0 h, the unstressed sample exhibits mask-edge defects extending ~70 nm deep as shown in Fig. 1(c) while the stressed specimen shows no mask-edge defects as displayed in Figs. 1(f) and 2(a). Small end of range (EOR) defects are observed near the original α/crystalline interface in all specimens.[22] The observations in mask-edge defect formation are the result of tensile [110] stresses with magnitude ~300 MPa induced in the substrate as predicted using simulations.[23] The [110] tensile stresses retard [110] SPE and prevent defect formation as presented elsewhere.[7–9] Interestingly, annealing for $t_{1.0}$=2.6 h in stressed specimens As^+-implanted at 7.5 keV produced mask-edge defects ~52 nm deep, as shown in Fig. 2(b). Thus, it is evident that the presence of As during SPE influences mask-edge defect formation.

The case of SPE at 525 °C with the addition of As^+-implantation at various energies in stressed (unetched) specimens is now considered. Figures 3(a)–3(c) present XTEM micrographs of the evolution of SPE in stressed samples additionally As^+-implanted at 7.5 keV. The predicted As concentration (C_{As}) profile is schematically superimposed on the as-implanted image in Fig. 3(a), which indicates R_p of ~10 nm.[21] After annealing for $t_{0.5}$=1.3 h, shown in the BF XTEM micrograph presented in Fig. 3(b), there is still significant separation of the [110] and [001] SPE fronts, presumably since the [001] α/crystalline interface did not approach the peak of the As profile. A small protrusion in the [110] α/crystalline interface near R_p (indicated by arrow) is evident, suggesting local SPE enhancement as indicated in Fig. 4(a). Annealing for $t_{1.0}$=2.6 h, shown in Fig. 3(c), reveals mask-edge defects ~52 nm deep.

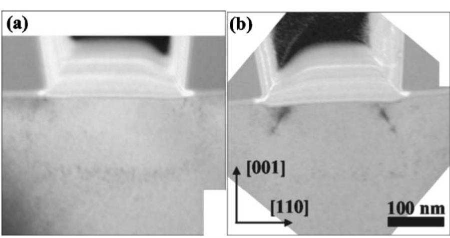

FIG. 2. BF XTEM images of samples annealed at 525 °C while stressed: (a) Si^+-implanted and annealed for $t_{1.0}$=3.0 h and (b) As^+-implanted at 7.5 keV and annealed for $t_{1.0}$=2.6 h.

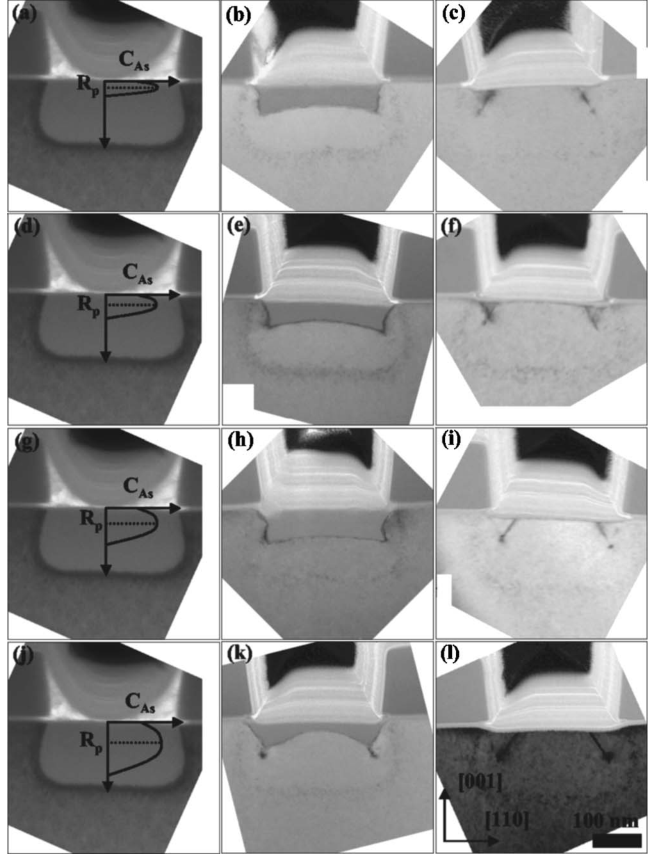

FIG. 3. BF XTEM images of As^+-implanted samples annealed at 525 °C while stressed, implanted at 7.5 keV: (a) as-implanted with concentration profile, (b) annealed for $t_{0.5}$=1.3 h, and (c) annealed for $t_{1.0}$=2.6 h; implanted at 15 keV: (d) as-implanted with concentration profile, (e) annealed for $t_{0.5}$=1.2 h, and (f) annealed for $t_{1.0}$=2.3 h; implanted at 30 keV: (g) as-implanted with concentration profile, (h) annealed for $t_{0.5}$=1.0 h, and (i) annealed for $t_{1.0}$=2.0 h; implanted at 50 keV: (j) as-implanted with concentration profile, (k) annealed for $t_{0.5}$=0.8 h, and (l) annealed for $t_{1.0}$=1.5 h.

Figures 3(d)–3(f) display XTEM micrographs of SPE occurring at 525 °C in stressed samples additionally As^+-implanted at 15 keV. A predicted R_p of ~16 nm is shown schematically in Fig. 3(d) on the image displaying the predicted As profile in the as-implanted structure.[21] The BF XTEM image of SPE completed to $t_{0.5}$=1.2 h, shown in Fig. 3(e), shows a small protrusion (indicated by an arrow) in the [110] α/crystalline interface near the R_p of the As, indicating a localized SPE enhancement. Completion of SPE after 2.3 h, shown in Fig. 3(f), reveals the existence of mask-edge defects at a depth of ~56 nm, similar to the 7.5 keV As^+-implanted specimen. It is interesting to note the smaller protrusion in the α/crystalline interface near R_p for the 7.5

Redistribution subject to AVS license or copyright; see http://scitation.aip.org/termsconditions. Download to IP: 130.56.106.27 On: Wed, 21 Oct 2015 04:11:12

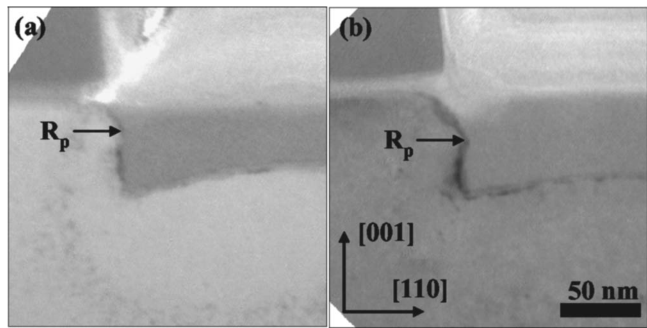

FIG. 4. BF XTEM images of As^+-implanted samples annealed at 525 °C while stressed: (a) implanted at 7.5 keV and annealed for $t_{0.5}=1.3$ h and (b) implanted at 30 keV and annealed for $t_{0.5}=1.0$ h.

keV As^+-implanted sample. This observation may be related to interface pinning at the $SiO_2/Si/\alpha$-Si boundary, which may have had a significant retarding effect near R_p for the 7.5 keV implant energy.[24]

Images depicting SPE evolution at 525 °C in stressed specimens additionally As^+-implanted at 30 keV are shown in Figs. 3(g)–3(i). Again, the predicted As profile is superimposed on the as-implanted structure, which indicates R_p of ~26 nm as shown in Fig. 3(g).[21] Annealing for $t_{0.5}=1.0$ h produced a very distinct protrusion in the [110] α/crystalline interface near R_p, again indicating a local SPE enhancement, as shown in Fig. 3(h). In this case, the protrusion (indicated by an arrow) is more pronounced compared to the 7.5 and 15 keV As^+-implanted samples, as shown in Fig. 4(b), presumably due to greater distance from the $SiO_2/Si/\alpha$-Si boundary. Completion of SPE after 2.0 h, shown in Fig. 2(i), reveals substantial mask-edge defects at a depth of ~56 nm, similar to the 15 keV As^+-implanted case.

Lastly, the sequence of SPE evolution at 525 °C in stressed samples additionally As^+-implanted at 50 keV is presented in Figs. 3(j)–3(l). The As profile superimposed on the as-implanted structure, presented in Fig. 3(j), indicates R_P of ~39 nm.[21] Annealing for $t_{0.5}=0.8$ h reveals that mask-edge defect formation has already commenced, as presented in Fig. 3(k). Completion of SPE after 1.5 h, shown in Fig. 3(l), reveals clear mask-edge defects with a depth of ~60 nm, similar to the other samples.

IV. DISCUSSION

Comparing the different As implants suggests that even with the application of stress from the patterning, the [110] SPE enhancement from the dopants is large enough to overcome the retardation from the stress, though the stress effect is not negligible as evidenced by the deeper defects observed in unstressed Si^+-implanted samples. Furthermore, the defect depth apparently is not very sensitive to As^+ implant energy. In the case of shallower As^+-implantation, the [001] regrowth front is far from R_p until it nears the surface and thus suffers minimal dopant enhancement. Correspondingly, the [110] SPE front is enhanced enough to produce an interface geometry favorable for defect formation, though it is somewhat retarded by the presence of the $SiO_2/Si/\alpha$-Si boundary.[24] In the case of deeper implantation, [001] SPE is enhanced at greater depths compared to shallower implantation. Meanwhile, the [110] front is less affected by the surface in this case and suffers greater enhancement. However, the enhancement to [001] SPE is great enough to keep the interface geometry unfavorable for defect formation until the regrowth process has partially completed. Thus, increasing the implant energy tends to enhance [001] SPE, which somewhat compensates for the enhanced [110] SPE. In contrast, decreasing the implant energy causes [110] SPE to be somewhat retarded by the presence of the surface, allowing the [001] front to regrow appreciably. This is evident in the XTEM images presented in Fig. 4.

It is interesting to note that no defects at the R_p of the implanted As were observed in any of the As^+-implanted samples, though the peak As concentration is well in excess of active solubility.[17] Furthermore, stress from the patterning did not influence the formation of these defects since none were observed in pattern-free specimens (not presented). Thus, it is likely that the As concentration was not high enough to form the extended defects and therefore it remains unknown what influence the formation of R_p defects has on mask-edge defect formation.

V. CONCLUSIONS

In summary, the influence of As^+-implantation on the formation of mask-edge defects during stressed solid phase epitaxy of two-dimensional amorphous Si regions created via ion-implantation was examined. The results indicated that the effect of stress on regrowth was much smaller than the enhancement generated via As^+-implantation, though the stress effect was not negligible. It was determined for a fixed peak As concentration of $\sim 5.0 \times 10^{20}$ cm^{-3} that increasing the As^+ implant energy did not significantly affect the depth of the mask-edge defects. This observation was attributed to localized enhancement in the [110] regrowth rate near the projected range of the As, which was retarded when the projected range was close to the surface or compensated by enhanced [001] SPE for a deeper projected range. Additionally, it appears the As concentration was not high enough to form defects at the As projected range and thus it is unknown what effect the formation of any projected range defects has on mask-edge defect formation.

ACKNOWLEDGMENTS

The authors wish to acknowledge The Semiconductor Research Corporation for funding this research.

[1]A. Bousetta, J. A. Vandenberg, R. Valizadeh, D. G. Armour, and P. C. Zalm, Nucl. Instrum. Methods Phys. Res. B **55**, 565 (1991).
[2]J. J. Hamilton, E. J. H. Collart, B. Colombeau, C. Jeynes, M. Bersani, D. Giubertoni, J. A. Sharp, N. E. B. Cowern, and K. J. Kirkby, Nucl. Instrum. Methods Phys. Res. B **237**, 107 (2005).
[3]J. Vonborany and R. Kogler, Nucl. Instrum. Methods Phys. Res. A **326**, 42 (1993).
[4]L. Csepregi, E. F. Kennedy, and T. W. Sigmon, J. Appl. Phys. **49**, 3906 (1978).
[5]H. Cerva and K.-H. Kusters, J. Appl. Phys. **66**, 4723 (1989).
[6]H. Cerva and W. Bergholz, J. Electrochem. Soc. **140**, 780 (1993).

Redistribution subject to AVS license or copyright; see http://scitation.aip.org/termsconditions. Download to IP: 130.56.106.27 On: Wed, 21 Oct 2015 04:11:12

[7]C. R. Olson, E. Kuryliw, B. E. Jones, and K. S. Jones, J. Vac. Sci. Technol. B **24**, 446 (2006).
[8]C. E. Ross and K. S. Jones, Mater. Res. Soc. Symp. Proc. **810**, C10.4.1 (2004).
[9]N. G. Rudawski, K. N. Siebein, and K. S. Jones, Appl. Phys. Lett. **89**, 082107 (2006).
[10]M. J. Aziz, P. C. Sabin, and G.-Q. Lu, Phys. Rev. B **44**, 9812 (1991).
[11]W. Barvosa-Carter and M. J. Aziz, Appl. Phys. Lett. **79**, 356 (2001).
[12]M. Horiuchi, M. Tamura, and S. Aoki, J. Appl. Phys. **65**, 2238 (1989).
[13]M. Tamura and M. Horiuchi, Jpn. J. Appl. Phys., Part 1 **27**, 2209 (1988).
[14]J. C. McCallum, Nucl. Instrum. Methods Phys. Res. B **148**, 350 (1999).
[15]B. C. Johnson and J. C. McCallum, J. Appl. Phys. **95**, 4427 (2004).
[16]L. Csepregi, E. F. Kennedy, T. J. Gallagher, J. W. Mayer, and T. W. Sigmon, J. Appl. Phys. **48**, 4234 (1977).
[17]D. Nobili, S. Solmi, A. Parisini, M. Derdour, A. Armigliato, and L. Moro, Phys. Rev. B **49**, 2477 (1994).
[18]O. Dokumaci, P. Rousseau, S. Luning, V. Krishnamoorthy, K. S. Jones, and M. E. Law, J. Appl. Phys. **78**, 828 (1995).
[19]S. N. Hsu and L. J. Chen, Appl. Phys. Lett. **55**, 2304 (1989).
[20]S. N. Hsu, L. J. Chen, and S. C. Wu, J. Appl. Phys. **68**, 4503 (1990).
[21]J. F. Ziegler, Nucl. Instrum. Methods Phys. Res. B **219–220**, 1027 (2004).
[22]K. S. Jones, S. Prussin, and E. R. Weber, Appl. Phys. A: Solids Surf. **A45**, 1 (1988).
[23]M. E. Law and S. M. Cea, Comput. Mater. Sci. **12**, 289 (1998).
[24]N. Burbure, N. G. Rudawski, and K. S. Jones, Electrochem. Solid-State Lett. **10**, H184 (2007).

Redistribution subject to AVS license or copyright; see http://scitation.aip.org/termsconditions. Download to IP: 130.56.106.27 On: Wed, 21 Oct 2015 04:11:12